SCIENCE CHINA Materials ARTICLES

mater.scichina.com link.springer.com

Published online 15 March 2018 | https://doi.org/10.1007/s40843-017-9232-2
Sci China Mater 2018, 61(9): 1201–1208

Humidity-responsive nanocomposite of gold nanoparticles and polyacrylamide brushes grafted on Ag film: synthesis and application as plasmonic nanosensor

Huaxiang Chen, Tingting You, Geng Xu, Yukun Gao, Chenmeng Zhang, Nan Yang and Penggang Yin*

ABSTRACT **A general stepwise strategy for the preparation of new humidity-responsive plasmonic nanosensor was described for the first time, based on Ag film functionalization by polyacrylamide (PAAM) brushes *via* surface-initiated atom transfer radical polymerization (SI-ATRP) method and then assembled with gold nanoparticles (Au NPs). We designed by this way a new plasmonic device made of Au NPs embedded in a humid vapor responsive polymer layer on Ag film and extensively characterized by surface-enhanced Raman scattering (SERS). When the relative humidity (RH) is above 50%, the number of plasmonic hotspots decreases, causing SERS signal reduced noticeably, for the volume expansion of PAAM brushes varied the nano-gap between closely spaced Au NPs, and between Au NPs and Ag film. The reversible optical properties of the prepared nanocomposite tuned by RH were probed through SERS using 4-mercaptopyridine (4-Mpy) as a molecular probe, and the decrease of the RH reversibly induces a significant enhancement of the 4-Mpy SERS signal. By means of the high reversibility, the RH responsive nanocomposite developed in this paper provides a dynamic SERS platform and can be applied as plasmonic nanosensor which is proved to be stable for at least two months.**

Keywords: RH-response, plasmonic nanosensor, SERS

INTRODUCTION

Metallic nanoparticles (NPs) are one of the most important and extensive family of materials in sensors, catalysis, semiconductors and medicine [1,2]. Surface-enhanced Raman scattering (SERS), known as one of the most powerful and sensitive tools for detection of molecules adsorbed onto metallic NPs, especially gold and silver [3–5], has been widely applied in the area of biology, optics and analytical chemistry [6–8]. In SERS, it is now well established that the signal enhancement is predominantly based on the plasmonic hotspots localized in the gaps (<10 nm) between closely spaced nanoparticles [9–11] or between a nanoparticle and a metal film [12–14]. Various approaches to create plenty of hotspots to raise high enhancement factors from SERS substrates have been reported recently [15,16]; however, due to the complex processes and high cost, it remains a challenge to fabricate uniform and stable SERS substrates with vast hotspots. Based on the previous studies, developing a simple method to assemble metallic NPs on metal surface with precise construction of plasmonic hotspots is of pivotal importance in fabricating efficient SERS substrates [17].

Recently, several strategies to stabilize metallic NPs on metal surfaces have been reported [18,19]. Furthermore, brushes of stimuli-responsive polymer, with unique structure and high diversity in functionalities, have been applied for the assembly of metal NPs on macroscopic surfaces with efficient control [20,21]. Sophisticated systems made of stimuli-responsive brushes assembled with gold or silver-NPs were proposed for SERS applications, with vast plasmonic hotspots formed under external stimulus [22–26]. For instance, Gehan *et al.* [27] reported that the SERS signals can be tuned by temperature stimulus, and the SERS substrate was prepared by using a thermo-responsive poly(*N*-isopropylacrylamide) (PNIPAM) brushes as linker between the gold NPs and a gold

Key Laboratory of Bio-inspired Smart Interfacial Science and Technology of Ministry of Education, School of Chemistry, Beihang University, Beijing 100191, China
* Corresponding author (email: pgyin@buaa.edu.cn)

 © Science China Press and Springer-Verlag GmbH Germany, part of Springer Nature 2018

film.

Inspired by humidity-responsive behaviors in nature, moisture responsive materials have awoken great interest for the applications in the area of nanosensors [28,29], actuators, or construction of soft robots [30]. However, to the best of our knowledge, fabrication of moisture responsive SERS substrates through the use of humidity-responsive polymer brushes grafted on a metal film to assemble Au NPs has barely been reported so far.

In this work, a general stepwise strategy to fabricate humid vapor responsive plasmonic nanosensor was described. Firstly, Ag-film was modified with binary self-assembled monolayers (SAMs) of an initiator and bis[2-(2-bromoisobutyryloxy)-undecyl] disulphide (DTBU) as an "inert" thiol to initiate the atom transfer radical polymerization (ATRP) of acrylamide (AAm), following which the Au NPs were assembled. Swelling of polyacrylamide (PAAM) brushes tuned by humid vapor is able to alter the distance not only between Au NPs and Ag film, but also among Au NPs, causing change of molecular probe's SERS signal. Most significantly, the SERS efficiency of the prepared SERS substrates could be remarkably modulated by relative humidity (RH) changing from 10% to 90%, using 4-mercaptopyridine (4-Mpy) as the model probe. When the RH was below 50%, the sensor was insensitiveness, with RH changing from 50% to 95%, the sensor has good sensitiveness. The prepared RH-responsive plasmonic nanosensor with good stability and homogeneity has attractive potential application in humidity probing mobile SERS micro sensors for their high moisture-responsive sensitivity and simple preparation process.

EXPERIMENTAL SECTION

Reagents

High-purity silver (99.99%, 10×10×0.25 mm^3) was purchased from Zhong Nuo Advanced Material (Beijing) Technology Co., Limited. Cu(I)Br, 1,1,4,7,7-pentamethyldiethylenetriamine (PMDETA), AAm (99.9%) and the initiator bis-DTBU was purchased from Sigma-Aldrich and used as received. 4-Mpy (99%), methanol (99.8%), ethanol (99.5%) and tetrahydrofuran (99.9%) were purchased from J&K Scientific. Deionized water was used throughout and obtained using a Millipore Direct-Q system.

Scheme 1 shows the fabrication of Ag film-PAAM-Au NPs nanocomposite, including a three-step procedure that consists of the following: (i) firstly, silver surface was modified with PAAM brushes *via* surface initiated-ATRP (SI-ATRP) method, and the chemical structure of Ag film-PAAM was confirmed by FT-IR spectrum, XPS and the contact angle, (ii) then, Au NPs were embedded into PAAM brushes grafted on Ag film, (iii) and lastly, after washed with water and dried in vacuum, the Ag-PAAM-Au NPs substrates were kept under nitrogen atmosphere.

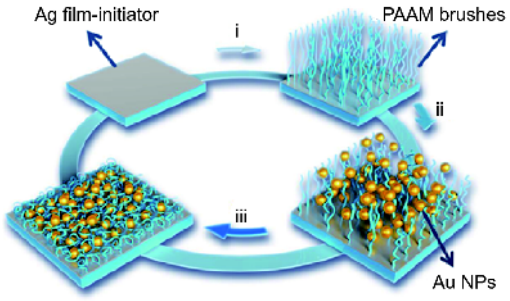

Scheme 1 Schematic illustration of the fabrication of PAAM brushes by ATRP on Ag film and immobilization of Au NPs.

Surface-initiated polymerization of acrylamide on Ag film

The Ag film was modified by DTBU initiator (H-NMR spectra of DTBU can be seen in Fig. S1). The silver substrate was rinsed by tetrahydrofuran, ethanol and water, and then dried in a nitrogen gas stream. Afterwards, the cleaned silver substrate was directly transferred into 1 mmol L^{-1} ethanol solution of ATRP initiator DTBU, kept immersed 12 h at 20°C. The initiator-modified silver surface was washed sequentially with THF and ethanol and dried in a stream of nitrogen before use.

PAAM brushes grafted on initiator-modified silver surface (Ag film-PAAM) were synthesized *via* the reported SI-ATRP method [31], and a reaction mixture of PMDETA (0.28 mL, 1.34 mmol), Milli-Q water, and methanol (3:7), AAm (2.00 g, 28.15 mmol), and CuBr (64 mg, 0.45 mmol) were used. In the beginning, the mixture of water and methanol was degassed and the chelating agent (PMDETA) was added. Under continuous stirring the monomer as well as the CuBr was added simultaneously to the solution under nitrogen gas flow. A three-necked flask was flushed with nitrogen, and the initiator-functionalized silver substrate was placed inside. Then the reaction mixture was transferred *via* a syringe to the three-necked flask which contained initiator-functionalized silver substrate, and the syringe was purged with nitrogen before used. After 6 h of reaction at 25°C, the substrate was rinsed and washed with Milli-Q water

 © Science China Press and Springer-Verlag GmbH Germany, part of Springer Nature 2018

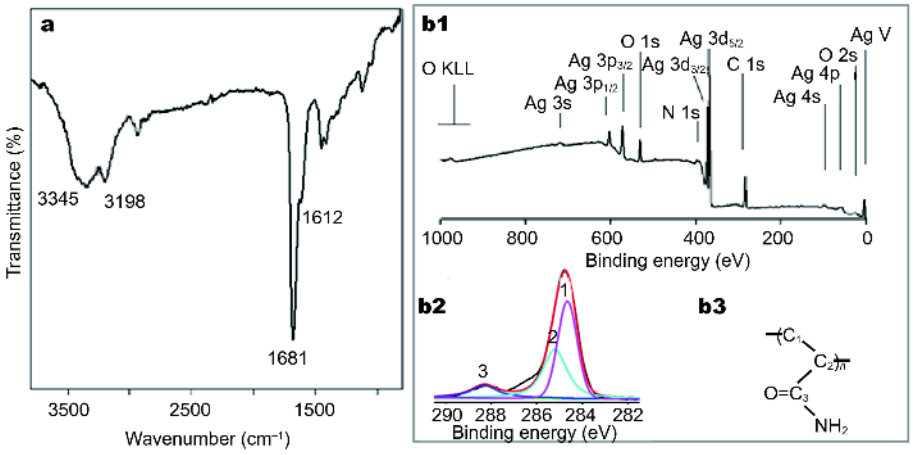

Figure 1 (a) FT-IR spectrum of the PAAM brushes coated on Ag-film; (b) XPS survey spectrum (b1) and C 1s core level spectrum of PAAM brushes grafted on silver substrate by means of ATRP (b2) and labeling of the different carbon moieties in a PAAM molecule (b3).

and ethanol, and then dried with a nitrogen gas stream.

Preparation of Au NPs-embedded polyacrylamide brushes grafted on Ag film

Au NPs with a diameter of 46 nm were synthesized successfully (Fig. S2). Three Ag film-PAAM substrates were separately soaked into the prepared Au NPs solution of 10 mL. Different loadings of Au NPs were embedded into PAAM brushes grafted on Ag film by controlling soaking time to 5 h, 10 h and 15 h. After reaction, the prepared Ag film-PAAM-Au NPs were taken out and rinsed with water, and then dried with a nitrogen gas stream.

RH adjustment

RH is achieved by adjusting the ratio of dry N_2 to water saturated N_2 (Fig. S6). RH is measured by hygrometer, and the ambient temperature is 20°C. Dry N_2 flow range is 0–5 mL min^{-1} and regulated by a nitrogen flow meter. Water-saturated N_2 is obtained by bubbling dry N_2 through water, and the dry N_2 flow range is 0–5 mL min^{-1}, regulated by a nitrogen flow meter.

SERS property of Ag film-PAAM-Au NPs substrate

The SERS activity of Ag film-PAAM-Au NPs substrate was studied using 4-Mpy as analyte. SERS samples were prepared by immersing Ag-PAAM-Au NPs substrates into 4-Mpy (1×10^{-5} mol L^{-1}, 10 mL) for 2 h before being rinsed with ethanol several times to remove the free molecules. The surface-enhanced Raman spectra were measured on an in Via-Reflex micro-Raman system (Renishaw, UK) equipped with a multi-channel charge-coupled device (CCD) detector and a confocal microscope (DM2500 M, Leica) using excitation by a 785 nm laser line.

Characterization

Fourier transform infrared (FTIR) spectra were collected on a Nicolet iN10 infrared spectrophotometer. The surface elemental compositions were obtained with an ESCA spectrometer (S-Probe ESCA SSX-100S, Surface Science Instruments, USA) with Al Kα X-ray radiation of 200 W. All elements present were identified from survey spectra (0−1,200 eV) with an energy resolution of 1.0 eV. The water contact angles with 2 μL water droplet were measured at ambient conditions using an optical contact angle meter (HARKE-CALS). Scanning electron microscopy (SEM) images were recorded by a JEOL JSM7500FA field emission microscope with an accelerating voltage of 5 kV. The acceleration voltage was increased to 10 kV for energy-dispersive X-ray analysis (EDX) measurements. Transmission electron microscopy (TEM) images were carried out using a JEOL JEM-2100F microscope with an accelerating voltage of 200 kV. The ultraviolet-visible absorption spectra (UV-vis) were measured on a Shimadzu UV-3150 spectrometer.

RESULTS AND DISCUSSION

In order to confirm the chemical structure of the prepared PAAM brushes coated on Ag film, samples were analyzed with FT-IR spectrum and X-ray photoelectron spectroscopy (XPS).

As shown in Fig. 1a, the strong bands at 3,345 and 3,198 cm^{-1} are related to N–H asymmetric and symmetric stretching of the NH_2 repeat unit, respectively [32]. The

 © Science China Press and Springer-Verlag GmbH Germany, part of Springer Nature 2018

strong peaks originating from the amide I band after Lorentz fitting were found at 1,681 cm^{-1}, and the amide II band was found at 1,612 cm^{-1}. As can be seen in Fig. 1b, the wide scan spectrum of PAAM brushes revealed the peaks corresponding to carbon, oxygen, and nitrogen atoms at characteristic binding energies. C 1s core level spectrum of the same sample has been deconvoluted into three component peaks. The intensity ratios of these deconvoluted peaks are in good agreement with the stoichiometric ratio of the corresponding carbon atoms in chemical structure of PAAM as [1]:[2]:[3]= 1:1:1. These results strongly confirm that the grafted polymer brush layer on Ag film is composed of PAAM chains.

It can be seen in Fig. 2, Ag film-PAAM surfaces were assembled with Au NPs effectively, and with the immobilization time changing from 5 to 15 h, the loadings of Au NPs increased obviously, and this result can also be confirmed by elemental maps of Au elements on the prepared three Ag film-PAAM-Au NPs substrates of 10×10 μm^2 (Fig. S5). With immobilization time of 10 h, uniformly dispersion of Au NPs on Ag film-PAAM was obtained, which can provide plenty of plasmonic hotspots.

By reducing the contact angle, the humidity sensitivity can be effectively increased. After modified by PAAM brushes with good moisture absorption, the contact angle of Ag film-PAAM surface changed from 65.2° to 21.7° (Fig. S3), confirming that the Ag film surface has been converted to hydrophilicity and good hygroscopicity by PAAM brushes. After Ag film-PAAM surface assembled with Au NPs, the surface roughness increased, causing the contact angle of Ag film-PAAM-Au NPs increased, as shown in Fig. 2. However, the surface of the prepared nanocomposite was still hydrophilic.

The prepared Ag film-PAAM-Au NPs were used as SERS substrates, on which 4-Mpy was adsorbed as target with a concentration of 1×10^{-5} mol L^{-1} in aqueous solution at 25°C. According to the previously reported SERS spectra of 4-Mpy on Ag and Au substrates [33], the two prominent peaks at 1,080 and 1,590 cm^{-1} are assigned to its aromatic ring breathing vibration.

As shown in Fig. 3a, the strongest SERS signal of 1×10^{-5} mol L^{-1} 4-Mpy adsorbed on Ag film-PAAM-Au NPs with immobilization time of 10 h was obtained, and in Fig. 3b, the smallest error bars of 4-Mpy SERS signal at 1,080 cm^{-1} was obtained in this condition, indicating that Ag film-PAAM with uniformly dispersion of Au NPs provided plenty of plasmonic hotspots which can be selected as SERS substrates with high sensitivity and good uniformity. While with immobilization time of 15 h, agglomeration of Au NPs on Ag film-PAAM was obtained, the plasmonic hotspots which localized in the gaps between closely spaced nanoparticles were reduced, causing and the SERS signal decreased. Furthermore, as shown in Fig. 3a (line a), no peaks corresponding to PAAM brushes (637, 764, 794, 1,105, 1,209, 1,328, 1,457, 1,625 cm^{-1}) [34] can be observed.

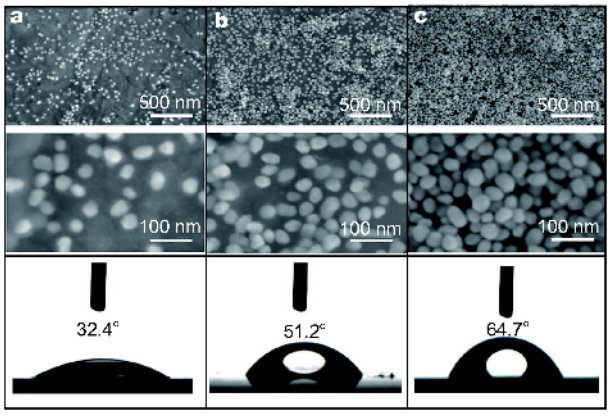

Figure 2 SEM images and the contact angle of Ag film-PAAM-Au NPs with immobilization time of 5 h (a), 10 h (b) and 15 h (c).

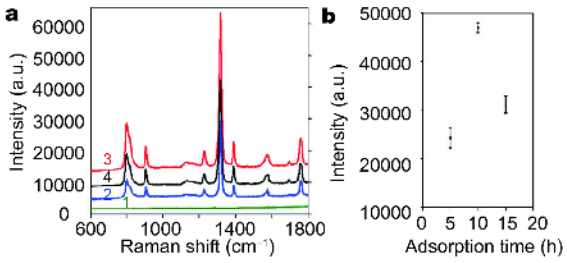

Figure 3 (a) Raman spectra of Ag film-PAAM-Au NPs (1), SERS spectrum of 1×10^{-5} mol L^{-1} 4-Mpy adsorbed on Ag film-PAAM-Au NPs with immobilization time of 5 h (2), 10 h (3) and 15 h (4). (b) The SERS intensity at 1080 cm^{-1} of 1×10^{-5} mol L^{-1} 4-Mpy adsorbed on Ag film-PAAM-Au NPs with different immobilization time, and the error bar is calculated with 5 repeats. The RH was 10%, and the acquisition time was 2 s.

Homogeneity of spectral signal through an area is of great importance when considering the practical application using SERS substrates [35]. As shown in Fig. 4, we performed a mapping measurement *via* spot to spot Raman spectra on a 20 μm×20 μm Ag film-PAAM-Au NPs area with a step size of 1 μm to evaluate the homogeneity of SERS signals at RH of 10%. SERS spectra of 4-Mpy obtained from different spots are with good stability. The relative standard deviation (RSD) of the Raman intensity was calculated to be 6.86% for 1,080 cm^{-1}, indicating the uniformity of SERS substrate in large area.

The prepared Ag film-PAAM-Au NPs can be used as

 © Science China Press and Springer-Verlag GmbH Germany, part of Springer Nature 2018

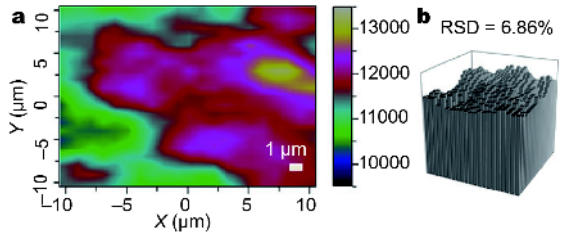

Figure 4 (a) Raman intensity mapping spectra at 1,080 cm^{-1} of 1×10^{-5} mol L^{-1} 4-Mpy molecules on a 20×20 μm^2 surface area of the Ag film-PAAM-Au NPs substrate, detected at the RH of 10% state and the acquisition time was 1 s. (b) The corresponding intensity distributions at 1,080 cm^{-1} of 4-Mpy molecules in (a).

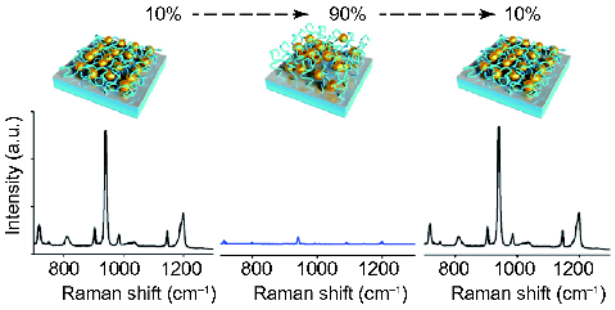

Figure 6 SERS spectra of 1×10^{-5} mol L^{-1} 4-Mpy adsorbed on Ag film-PAAM-Au NPs, detected at various RH: from 10% to 90% and back to 10%. The acquisition time was 2 s.

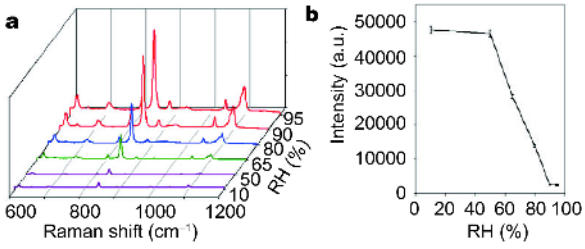

Figure 5 (a) SERS spectra recorded at various RH of 1×10^{-5} mol L^{-1} 4-Mpy molecules adsorbed on Ag film-PAAM-Au NPs. (b) Integrated SERS intensity at 1,080 cm^{-1} of 4-Mpy molecules adsorbed on Ag film-PAAM-Au NPs under various RH, the error bar is calculated with 5 repeats.

humidity-responsive plasmonic nanosensor, and the relationship between humidity and SERS signal of 4-Mpy adsorbed on Ag-PAAM-Au NPs was studied in detail. The ambient RH around SERS substrates can be tuned easily by regulating the gas ratio between dry N_2 and water saturated N_2, and the SERS signal of 1×10^{-5} mol L^{-1} 4-Mpy adsorbed on the SERS substrates under different ambient RH can be detected efficiently (Fig. S6).

Fig. 5a illustrated the effect of RH changes from 10% to 95% on the strength of SERS signal. In Fig. 5a, in the range from 10% to 50% RH, the SERS signal of 4-Mpy adsorbed on Ag film-PAAM-Au NPs basically remained unchanged, for that hygroscopic expansion of PAAM brushes did not occur. The synergistic effect caused by the SERS hotspots among closely spaced Au NPs, and between Au NPs and Ag film, can enhance SERS intensity obviously [36–37]. With the increase of RH from 50% to 90%, volume expansion occurs when the PAAM brush absorbs moisture, increasing the nano-gap among Au NPs, and the distance between Au NPs and Ag film. As a result, the number of plasmonic hotspots reduced sharply and the SERS signal strength decreased obviously. Good repeatability can be obviously seen from Fig. 5b when repeated regulation RH from 10% to 95% five times.

Furthermore, as shown in Fig. 6, it is remarkable that the variations of the SERS intensities observed for Ag film-PAAM-Au NPs are fully reversible when turning RH from 10% to 90% and back to 10%, evidencing a strong and reversible response of the Ag film-PAAM-Au NPs system to the external RH. The number of plasmonic hotspots located in the nano-gap among Au NPs, and between Au NPs and Ag film can be reversible altered efficiently by tuning external RH. These phenomena indicate that the fabricated humidity-responsive plasmonic nanosensor can response to the change of the surrounding media from low RH to high RH state and *vice versa*.

SERS signals caused by plasmonic hotspots can be quantified by enhancement factors (EF). To compare the enhancement more quantitatively, we have calculated the EFs for the main Raman peaks of 4-Mpy adsorbed on Ag film-PAAM-Au NPs, as shown in Fig. 7, based on the reported method [38]: $EF=(I_{SERS}/N_{ads})/(I_{bulk}/N_{bulk})$ (Equation (1)), where I_{SERS} and I_{bulk} are the SERS intensities of 1×10^{-5} mol L^{-1} 4-Mpy adsorbed on Ag-PAAM-Au NPs and normal Raman spectra of 5 mol L^{-1} 4-Mpy adsorbed on Si wafer at the 1,080 cm^{-1} band, respectively; N_{bulk} and N_{ads} are the number of 4-Mpy molecules under the same laser illumination conditions for the bulk and SERS experiments, respectively. By substituting values into Equation (1), EF for the SERS of 4-Mpy adsorbed on Ag film-PAAM-Au NPs was estimated to be 2×10^{8}.

As can be seen from Fig. 8, the SERS signal of 1×10^{-5} mol L^{-1} 4-Mpy did not change after two months at RH of 10% or 90%, proving that the Ag film-PAAM-Au NPs SERS substrate was stable for at least two months, and the SERS intensities can be fully reversible with RH varying from 10% to 90% after two months.

 © Science China Press and Springer-Verlag GmbH Germany, part of Springer Nature 2018

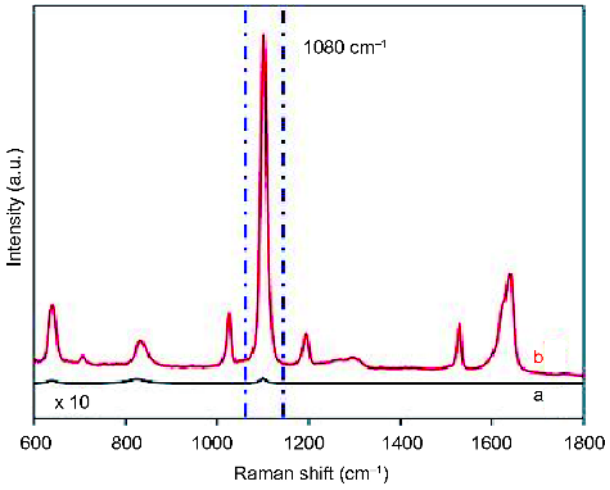

Figure 7 (a) Normal Raman spectrum of 5 mol L^{-1} 4-Mpy adsorbed on Si wafer. (b) SERS spectrum of 1×10^{-5} mol L^{-1} 4-Mpy adsorbed on Ag film-PAAM-Au NPs, detected at the RH of 10% and the acquisition time was 2 s.

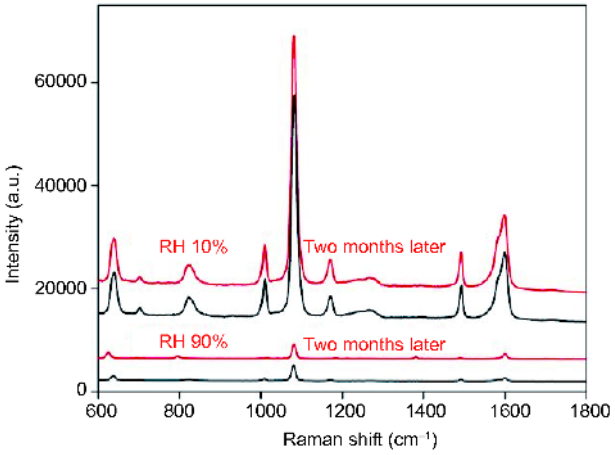

Figure 8 The SERS spectra of 1×10^{-5} mol L^{-1} 4-Mpy adsorbed on Ag film-PAAM-Au NPs after two months, detected at the RH of 10% and 90% state and the acquisition time was 2 s.

CONCLUSIONS

In summary, a novel humidity-responsive plasmonic nanosensor was successfully fabricated by a two-step strategy: PAAM-modified Ag film was firstly prepared by SI-ATRP method, after which Au NPs were embedded into PAAM brushes. The prepared PAAM brushes coated on Ag film were confirmed by FTIR and XPS. With Au NPs immobilization time of 10 h, Ag film-PAAM-Au NPs nanocomposite with uniformly dispersion of Au NPs was obtained, and at RH of 10%, the strongest SERS signal of 1×10^{-5} mol L^{-1} 4-Mpy adsorbed on the substrate was observed, and moreover, the RSD for a mapping SERS measurement of 4-Mpy was calculated to be 6.86% on a 20 μm×20 μm area, indicating the uniformity of SERS substrate in large area. Meanwhile, the nanocomposite with good moisture sensitivity was successfully prepared, with the contact angle of 51.2°.

With the prepared nanocomposite as humidity-responsive plasmonic nanosensor, the relationship between RH and SERS signal of 4-Mpy adsorbed on Ag-PAAM-Au NPs was studied in detail. At the RH below 50%, volume expansion of the PAAM brushes did not occurr, and thus the prepared nanosensor was insensitive. When the RH is above 50%, the number of plasmonic hotspots decreases, because the volume expansion of the PAAM brushes varied the nano-gap between closely spaced Au NPs, and between Au NPs and Ag film, causing SERS signal reduced obviously. Turning RH from 10% to 90% and back to 10%, the variations of the SERS intensities are fully reversible. Furthermore, at RH of 10%, EFs for the SERS signal of 4-Mpy adsorbed on Ag film-PAAM-Au NPs, caused by plasmonic hotspots, was estimated to be 2×10^{8}. The SERS intensities can be fully reversible with RH varying from 10% to 90% for several months. The fabricated humidity-responsive plasmonic nanosensors can response to the change of the surrounding media from low RH to high RH state and *vice versa*.

Received 18 December 2017; accepted 13 February 2018; published online 15 March 2018

1 Ferrando R, Jellinek J, Johnston RL. Nanoalloys: from theory to applications of alloy clusters and nanoparticles. Chem Rev, 2008, 108: 845–910
2 Yang Y, Jiang X, Chao J, *et al.* Synthesis of magnetic core-branched Au shell nanostructures and their application in cancer-related miRNA detection *via* SERS. Sci China Mater, 2017, 60: 1129–1144
3 Gersten J, Nitzan A. Electromagnetic theory of enhanced Raman scattering by molecules adsorbed on rough surfaces. J Chem Phys, 1980, 73: 3023–3037
4 Dieringer JA, Wustholz KL, Masiello DJ, *et al.* Surface-enhanced Raman excitation spectroscopy of a single rhodamine 6G molecule. J Am Chem Soc, 2009, 131: 849–854
5 Duan C, Ren B, Liu H, *et al.* Flexible SERS active detection from novel Ag nano-necklaces as highly reproducible and ultrasensitive tips. Sci China Mater, 2016, 59: 435–443
6 Lin J, Shang Y, Li X, *et al.* Ultrasensitive SERS detection by defect engineering on single Cu_2O superstructure particle. Adv Mater, 2017, 29: 1604797
7 Stiles PL, Dieringer JA, Shah NC, *et al.* Surface-enhanced Raman spectroscopy. Annu Rev Anal Chem, 2008, 1: 601–626
8 Wang M, Meng G, Huang Q, *et al.* CNTs-anchored egg shell membrane decorated with Ag-NPs as cheap but effective SERS substrates. Sci China Mater, 2015, 58: 198–203
9 Chen SY, Lazarides AA. Quantitative amplification of Cy5 SERS in 'warm spots' created by plasmonic coupling in nanoparticle assemblies of controlled structure. J Phys Chem C, 2009, 113: 12167–

 © Science China Press and Springer-Verlag GmbH Germany, part of Springer Nature 2018

12175
10 Guerrini L, McKenzie F, Wark AW, *et al.* Tuning the interparticle distance in nanoparticle assemblies in suspension *via* DNA-triplex formation: correlation between plasmonic and surface-enhanced Raman scattering responses. Chem Sci, 2012, 3: 2262
11 Qian X, Li J, Nie S. Stimuli-responsive SERS nanoparticles: conformational control of plasmonic coupling and surface Raman enhancement. J Am Chem Soc, 2009, 131: 7540–7541
12 Gupta S, Agrawal M, Uhlmann P, *et al.* Gold nanoparticles immobilized on stimuli responsive polymer brushes as nanosensors. Macromolecules, 2008, 41: 8152–8158
13 Kim NH, Lee SJ, Moskovits M. Aptamer-mediated surface-enhanced Raman spectroscopy intensity amplification. Nano Lett, 2010, 10: 4181–4185
14 Mubeen S, Zhang S, Kim N, *et al.* Plasmonic properties of gold nanoparticles separated from a gold mirror by an ultrathin oxide. Nano Lett, 2012, 12: 2088–2094
15 Tang H, Meng G, Huang Q, *et al.* Arrays of cone-shaped ZnO nanorods decorated with Ag nanoparticles as 3D surface-enhanced Raman scattering substrates for rapid detection of trace polychlorinated biphenyls. Adv Funct Mater, 2012, 22: 218–224
16 Lim DK, Jeon KS, Hwang JH, *et al.* Highly uniform and reproducible surface-enhanced Raman scattering from DNA-tailorable nanoparticles with 1-nm interior gap. Nat Nanotechnol, 2011, 6: 452–460
17 Gupta S, Agrawal M, Conrad M, *et al.* Poly(2-(dimethylamino) ethyl methacrylate) brushes with incorporated nanoparticles as a SERS active sensing layer. Adv Funct Mater, 2010, 20: 1756–1761
18 Agrawal M, Pich A, Zafeiropoulos NE, *et al.* Polystyrene–ZnO composite particles with controlled morphology. Chem Mater, 2007, 19: 1845–1852
19 Nie G, Li G, Wang L, *et al.* Nanocomposites of polymer brush and inorganic nanoparticles: preparation, characterization and application. Polym Chem, 2016, 7: 753–769
20 Gupta S, Agrawal M, Uhlmann P, *et al.* Poly(*N*-isopropyl acrylamide)–gold nanoassemblies on macroscopic surfaces: fabrication, characterization, and application. Chem Mater, 2010, 22: 504–509
21 Li Y, Bai X, Xu M, *et al.* Photothermo-responsive Cu_7S_4@polymer nanocarriers with small sizes and high efficiency for controlled chemo/photothermo therapy. Sci China Mater, 2016, 59: 254–264
22 Sánchez-Iglesias A, Grzelczak M, Rodríguez-González B, *et al.* Synthesis of multifunctional composite microgels *via in situ* Ni growth on pNIPAM-coated Au nanoparticles. ACS Nano, 2009, 3: 3184–3190
23 Mistark PA, Park S, Yalcin SE, *et al.* Block-copolymer-based plasmonic nanostructures. ACS Nano, 2009, 3: 3987–3992
24 Gupta S, Uhlmann P, Agrawal M, *et al.* Immobilization of silver nanoparticles on responsive polymer brushes. Macromolecules, 2008, 41: 2874–2879
25 Oren R, Liang Z, Barnard JS, *et al.* Organization of nanoparticles in polymer brushes. J Am Chem Soc, 2009, 131: 1670–1671
26 Tokareva I, Minko S, Fendler JH, *et al.* Nanosensors based on responsive polymer brushes and gold nanoparticle enhanced transmission surface plasmon resonance spectroscopy. J Am Chem Soc, 2004, 126: 15950–15951
27 Gehan H, Fillaud L, Chehimi MM, *et al.* Thermo-induced electromagnetic coupling in gold/polymer hybrid plasmonic structures probed by surface-enhanced Raman scattering. ACS Nano, 2010, 4: 6491–6500
28 Lv C, Xia H, Shi Q, *et al.* Sensitively humidity-driven actuator based on photopolymerizable PEG-DA films. Adv Mater Interfaces, 2017, 4: 1601002
29 Han DD, Zhang YL, Jiang HB, *et al.* Moisture-responsive graphene paper prepared by self-controlled photoreduction. Adv Mater, 2015, 27: 332–338
30 de Volder M, Tawfick SH, Copic D, *et al.* Hydrogel-driven carbon nanotube microtransducers. Soft Matter, 2011, 7: 9844–9847
31 Dong R, Krishnan S, Baird BA, *et al.* Patterned biofunctional poly(acrylic acid) brushes on silicon surfaces. Biomacromolecules, 2007, 8: 3082–3092
32 Kong X, Kawai T, Abe J, *et al.* Amphiphilic polymer brushes grown from the silicon surface by atom transfer radical polymerization. Macromolecules, 2001, 34: 1837–1844
33 Michota A, Bukowska J. Surface-enhanced Raman scattering (SERS) of 4-mercaptobenzoic acid on silver and gold substrates. J Raman Spectrosc, 2003, 34: 21–25
34 Gupta MK, Bansil R. Laser Raman spectroscopy of polyacrylamide. J Polym Sci Polym Phys Ed, 1981, 19: 353–360
35 Jiang L, Liang X, You T, *et al.* A sensitive SERS substrate based on Au/TiO_2/Au nanosheets. Spectrochim Acta Part A-Mol Biomol Spectr, 2015, 142: 50–54
36 Sun M, Qian H, Liu J, *et al.* A flexible conductive film prepared by the oriented stacking of Ag and Au/Ag alloy nanoplates and its chemically roughened surface for explosive SERS detection and cell adhesion. RSC Adv, 2017, 7: 7073–7078
37 Qian H, Xu M, Li X, *et al.* Surface micro/nanostructure evolution of Au–Ag alloy nanoplates: Synthesis, simulation, plasmonic photothermal and surface-enhanced Raman scattering applications. Nano Res, 2016, 9: 876–885
38 Zhang L, Jiang C, Zhang Z. Graphene oxide embedded sandwich nanostructures for enhanced Raman readout and their applications in pesticide monitoring. Nanoscale, 2013, 5: 3773–3779

Acknowledgements This work was supported by the National Natural Science Foundation of China (51572009).

Author contributions You T, Xu G and Gao Y designed and supervised the project. Chen H carried out the experiments with assistance from Zhang C, Yang N and Yin P. Chen H, You T and Yin P wrote the manuscript. All authors discussed the results and commented on the manuscript at all stages.

Conflict of interest The authors declare no conflict of interest.

Supplementary information Supporting data are available in the online version of the paper.

 © Science China Press and Springer-Verlag GmbH Germany, part of Springer Nature 2018

Huaxiang Chen is a PhD student at the School of Chemistry, Beihang University, under the supervision of Prof. Penggang Yin. Currently, he is working on the development of environmental-sensitive SERS nanosensors.

Penggang Yin is a professor at the School of Chemistry, Beihang University. He obtained his PhD in 2003 from Beijing Institute of Technology. From 2003 to 2005, he worked as a postdoctoral fellow at Institute of Semiconductors, Chinese Academy of Sciences. He has worked at Beihang University since 2005 with research interests focusing on Raman spectroscopy and surface-enhanced Raman spectroscopy, fabrication, characterization and numerical simulation of nanomaterial.

湿度响应纳米复合材料的组装及其SERS传感器应用

陈华祥, 尤汀汀, 徐更, 高宇坤, 张晨萌, 杨楠, 殷鹏刚*

摘要 本文报道了一种湿度响应纳米SERS传感器. 通过原子转移自由基聚合技术在银片表面嫁接了具有湿度响应性能的聚丙烯酰胺分子刷, 并组装金纳米颗粒形成复合结构. 该分子刷湿度响应灵敏, 而且可有效抓取金纳米颗粒, 构成均匀分布的SERS“热点”. 通过调节湿度, 实现了SERS“热点”的可逆调控, 并通过拉曼光谱快速捕捉探针分子特征峰的SERS信号强度变化, 实现湿度响应的SERS传感功能. 湿度低于50%时, 分子刷收缩, 金纳米颗粒间距降至纳米级, 形成大量热点, 使得SERS增强因子达到2×10^8; 湿度高于50%时, 分子刷舒张, 金纳米颗粒间距变大, 当湿度大于90%时, SERS“热点”最少, SERS信号最低. 可逆调控湿度变化, 得到可逆的SERS信号变化, 因此该复合材料实现了高效灵敏的湿度响应SERS传感.

 © Science China Press and Springer-Verlag GmbH Germany, part of Springer Nature 2018